doi:10.1006/jmbi.2000.4430 available online at http://www.idealibrary.com on IDEAL® *J. Mol. Biol.* (2001) **306**, 727–732

JMB

pH-induced Structural Changes Regulate Histidine Decarboxylase Activity in *Lactobacillus* 30a

Elisabeth Schelp, Scott Worley, Arthur F. Monzingo, Stephen Ernst and Jon D. Robertus*

Institute of Cellular and Molecular Biology, Department of Chemistry and Biochemistry University of Texas, Austin TX 78712, USA

**Corresponding author*

Histidine decarboxylase (HDC) from *Lactobacillus* 30a produces histamine that is essential to counter waste acids, and to optimize cell growth. The HDC trimer is active at low pH and inactive at neutral to alkaline pH. We have solved the X-ray structure of HDC at pH 8 and revealed the novel mechanism of pH regulation. At high pH helix B is unwound, destroying the substrate binding pocket. At acid pH the helix is stabilized, partly through protonation of Asp198 and Asp53 on either side of the molecular interface, acting as a proton trap. In contrast to hemoglobin regulation, pH has a large effect on the tertiary structure of HDC monomers and relatively little or no effect on quaternary structure.

Keywords: histidine decarboxylase; helix disorder, pH regulation; X-ray; pyruvoyl

Introduction

Lactobacilli are lactic acid producing bacteria; they grow best at pH values between 5 and 6.5 but their metabolism can lower the environmental pH to about 4, where growth stops. In the presence of histidine, wild-type *L.* 30a strains synthesize and secrete histamine that counters the lowering of pH and allows denser growth than for mutant strains lacking histidine decarboxylase (HDC) activity.[1] The histamine is a product of a pH-regulated HDC which converts histidine to histamine and CO_2. The product histamine is involved in an energy producing histidine/histamine antiport mechanism.[2] One proton is removed from the cytoplasm, raising the pH, and creating an electrostatic gradient that can be used for ATP synthesis. HDC is a vital component of this system, chemically sensing when pH and substrate levels require the decarboxylation of histidine.

The biochemical properties of HDC from *L.* 30a have been intensely studied by Snell and his co-workers.[3] HDC uses a covalently bound pyruvoyl moiety as an electron sink in the decarboxylation reaction. The pyruvate cofactor is formed as HDC undergoes an autoactivation serinolysis reaction in which an inactive chain of 310 amino acid residues is cleaved to produce an 81-residue β chain and a 228-residue α chain with the pyruvoyl group at its amino terminus.[4] The 2.5 Å X-ray structure of HDC has been solved at pH 4.8.[5,6] HDC forms a cup-shaped trimer with a deep central cavity containing three active sites. Each active site is formed at the interface between two monomers of the trimer. Two trimers can form weak tail-to-tail interactions to form a hexamer,[7] but the hexamer is unlikely to have any catalytic significance. Homologs of the *L.* 30a HDC exist as trimers and also exhibit the same kinetic patterns as the *L.* 30a enzyme.[8]

The structure of HDC complexed with the inhibitor histidine methyl ester (HME) has been solved allowing for the identification of potential active site residues.[9] The *hdc* gene has been moved to a high yield expression vector,[10] facilitating the investigation by site-directed mutagenesis of essentially all of the amino acid residues identified as being mechanistically important.[11-14]

HDC has been shown to have greatly reduced activity at neutral or alkaline pH. This is largely a substrate binding effect in that the enzyme has a K_m of 0.3 mM at pH 4.8 and 100 mM at pH 7.[15] The X-ray model at pH 4.8[5,6] represents the active form of HDC; here we present the structure of the less active form of HDC at pH 8 (HDC-8).

Abbreviations used: HDC, histidine decarboxylase; HME, histidine methylester.

E-mail address of the corresponding author: jrobertus@mail.utexas.edu

0022-2836/01/040727–6 $35.00/0

Results and Discussion

At pH 4.8, HDC crystallizes in space group $I4_122$ with the asymmetric unit being a trimer of 310 amino acid monomers.[5,7] Two trimers, related by a crystallographic 2-fold, form a weak tail-to-tail hexamer. At pH 8, HDC crystallizes in space group *R*32, and the asymmetric unit was found to be a tail-to-tail dimer composed of two 310 amino acid monomers. This corresponds to one-third of the previously observed HDC hexamer unit with the crystallographic 3-fold relating the tail-to-tail dimers in the hexamer. Table 1 shows the crystallographic data summary for HDC-8. After 11 rounds of refinement, the crystallographic working *R*-factor was 0.25 and the free *R*-factor was 0.31. The model deviates (rms) from standard bond lengths and angles by 0.012 Å and 3.027°, respectively. 87.4% of residues lie in the favored and allowed regions of the Ramachandran plot. 1.4% are in the generously allowed region and Gln22 and Asn69 are in the disallowed region. These residues are also in the disallowed region in the pH 4.8 structure and this suggests they are truly strained in the folding of the protein.[6]

The overall fold of the pH 8 protein strongly resembles that of the pH 4.8, active, model.[6] The rms deviation among all visible C_αs is 0.9 Å. The quaternary structure is also conserved. That is, the crystallographically related trimers of HDC-8 do not expand or contract radially from the molecular 3-fold axis seen in the pH 4.8 structure, nor do the subunits shear with respect to one another.

The only significant difference in structure between the active pH 4.8 and the inactive HDC-8 forms is that residues 49 to 63 are disordered in HDC-8. What has been referred to as helix B in the active form contains residues 53 to 68.[6] In HDC-8, residues 64 to 68 maintain helical parameters, but helix B residues 53 to 63 are disordered and have no electron density. In addition, loop residues 49 to 52 are also disordered. There are no crystal packing contacts involving residues 49 to 64 in the pH 4.8 structure which could induce ordering. Likewise, there are no packing contacts in the pH 8 structure which would cause the B helix and its preceding loop to disorder.

Table 1. Crystallographic data

Space group: *R*32 Cell parameters: *a*=117.4, *b*=117.4, *c*=241.6 Å, α=β=90, γ=120	
Resolution (Å)	2.7
R_{merge} (%)	5.3
R_{merge} (last shell) (%)	21.1
I/σ	29.9
I/σ (last shell)	7.3
Completeness (%)	98.4
Unique reflections	17,625
Redundancy	4.2
$R_{working}$	0.25
R_{free}	0.31
RMS deviation of model From ideal bond	
Lengths (Å)	0.012
Angles (deg.)	3.027

Figure 1(a) shows a 2.7 Å electron density map for a helical region (residues 281 to 288) of the refined protein structure. This region has no particular structural significance, except that it is part of a protein surface helix of about the same size as the B helix. This Figure shows that the HDC-8 electron density map in other regions of the model is of high quality, that the molecular model can generally be fit with confidence, and the map would reveal the existence of any stable helix. As shown in Figure 1(b), the absence of similar, or any, interpretable density for residues 49 to 63 indicates that they are truly disordered in HDC-8.

The role of helix B in substrate binding has been implicated in the observed binding of the substrate analog HME to wild-type HDC.[9] This is indicated in Figure 2, which shows two monomers of an HDC trimer, viewed from the inside of the trimer. The interface between the two contains one active site contributed to by both monomers. In the trimer, two additional sites would be formed around the trimeric ring. Figure 2 shows the wild-type, active, form of HDC where the ordered loop and B helix (residues 49 to 64) of the right hand monomer are shown in black. The binding of HME is shown attached to the pyruvoyl group of the left hand monomer. It is clear that in the active form, helix B on one monomer can interact with the substrate formally sitting in the adjacent monomer.

Figure 3 is a cartoon representation of an HDC active site region with key residues from the two contributing monomers identified. The monomer on the left contains catalytic groups Glu197 and the pyruvoyl cofactor (Pyr82). The cofactor forms a Schiff base with the histidine substrate, shown in dark bonds, while E197 protonates the intermediate to facilitate decarboxylation.[11] The monomer on the right in the Figure forms the other half of the active site, concerned largely with substrate binding. In the active form, illustrated here, it contributes important substrate-binding residues that all lie on helix B. These key substrate binding residues include Ile59′, Tyr62′, and Asp63′ (the primes indicate that the residues lie on the second monomer). When the substrate analog HME binds to HDC, Ile59′ moves 1.5 Å and Tyr62′ rotates 30° to contact the substrate through a chain of hydrogen bonds.[9] It is also known that Asp63′ forms an ion pair with the substrate imidazolium; conversion to Asn (D63N) increases K_m 240-fold.[13]

The electron density map for the HDC-8 protein shows, however, that residues 49 to 63 are disordered and cannot be modeled. In Figure 3, the labels R48′ and R64′ indicate the boundary of the disordered region. As a consequence of the disorder, none of the three substrate-binding residues discussed above has a defined position in HDC-8. It is clear that high pH disorders, or melts, the B helix and destroys one half of the active site. This

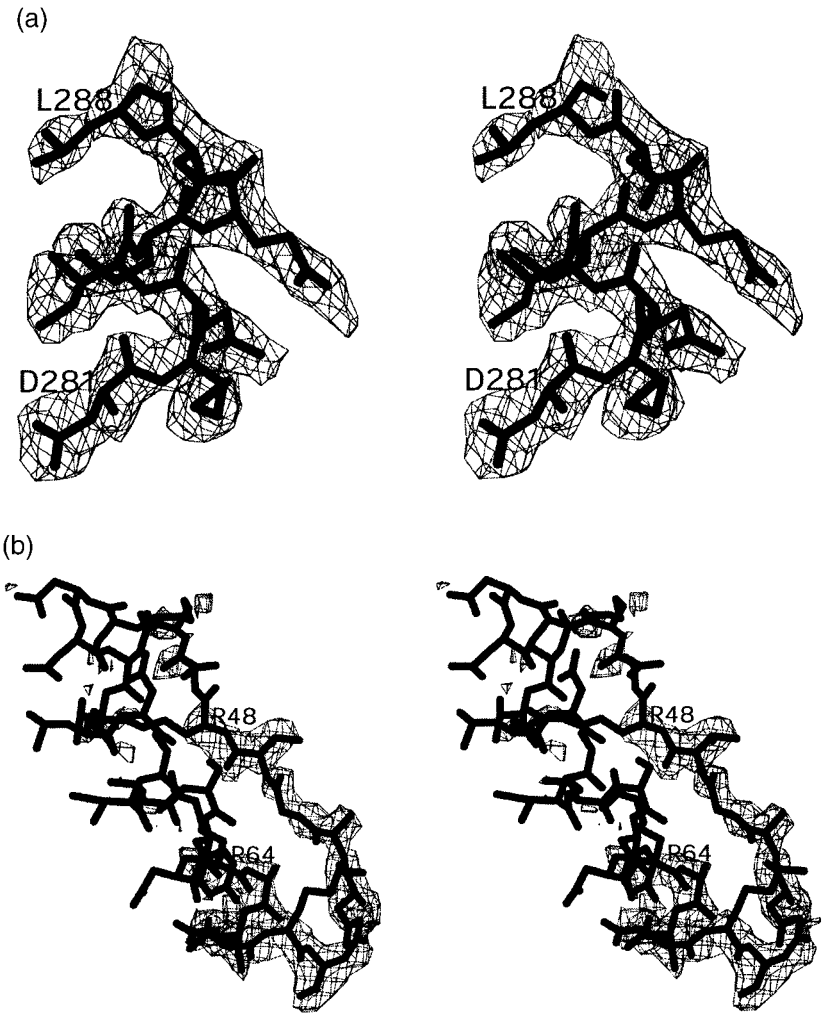

Figure 1. Electron density for the HDC-8 crystal. (a) A portion of an extended α-helix containing residues 281 to 288 is shown. (b) The electron density for residues 44 to 69 is shown with corresponding model from the pH 4.8 structure superimposed. The map was calculated with $2F_o - F_c$ amplitudes and LBEST weighted phases. The electron density basket is contoured at 0.9 σ.

in turn, accounts for the high K_m and low activity observed at neutral to alkaline pH.[13]

The mechanism of HDC activity regulation by pH is novel. To analyze the pH-dependent triggering of the mechanism, we can compare the active and inactive structures. The active, low pH, structure has short, strong, hydrogen bonds across the intermolecular interface between the side-chains of Asp198 of one monomer and Asp53′ of a neighboring monomer.[6] This interaction is indicated in Figure 3.

It has been proposed that this hydrogen-bonding pair constitutes the major part of a pH regulating ''proton trap''.[14] Protonating the pair of carboxylates at low pH neutralizes their repulsive negative charges and allows them to form the observed hydrogen-bonded pair. The free energy difference between the disordered and ordered states of peptide segment 49′-63′ must be small enough that the hydrogen bonds of the protonated 198 and 53′ residues can stabilize the ordered structure, including the B helix.

The role of Asp198 and Asp53′ in the pH regulation of activity is confirmed by site-directed mutagenesis. Converting these two residues to asparagine abolishes the pH regulation of the enzyme.[14] Although the replacement amides of the double mutant should be able, in principle, to hydrogen bond to one another and form a version of the proton trap, the bonds between them may not be strong enough to fully anchor the protein in the active form. The double mutant has the same k_{cat} as the wild-type enzyme but the apparent K_m is increased 13-fold.[14] This is consistent with the notion that the substrate binding pocket of the double mutant is not perfectly formed and the B helix may be partially disordered.

The classic case of proton regulation of protein activity through pH-induced structural change is hemoglobin. Hemoglobin affinity for oxygen is a function of pH as observed in the Bohr effect. The structural mechanism is sophisticated but has been broken down into several component parts.[16] For example, it is known that in the T (deoxy) state His146 of the β chain forms an ion pair with Asp94 and this helps stabilize the T state structure. At higher pH, His146 deprotonates, the ion pair is ruptured, and the structure is driven toward the R (oxy) state. In hemoglobin, the proton regulation works largely through small tertiary rearrange-

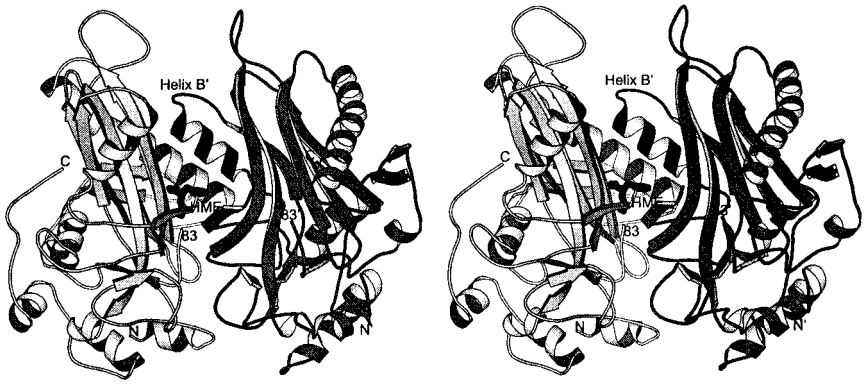

Figure 2. The structure of HDC. Two HDC monomers are shown. The molecule on the left is shaded a light tone and that on the right is darker. The N and C termini are indicated as are residues 83 which bind the pyruvoyl cofactors and represent the amino terminus of the larger chain of each activated monomer. The position that would be occupied by the substrate analog HME is indicted in the left monomer. Helix B′ of the right monomer, and the loop leading into it, are shaded black and the helix is labeled. The position for helix B shown is that seen in the low pH, active, enzyme but this helix is disordered in HDC-8. The Figure was generated using MOLSCRIPT.[26]

ments that accumulate to trigger a large change in the quaternary structure. In the case of HDC, the effect of proton binding is dramatic at the tertiary structural level but the overall quaternary rearrangement for HDC is negligible.

Helix order/disorder transitions are part of the control of activity for the G factor, Giα1, triggered by phosphate interactions.[17] GTP binds to this protein to activate it. In the active form, ionic and hydrogen bonding interactions between the γ-phosphate of GTP and the enzyme stabilize the α2 helix in the switch II region of the enzyme. The helix positions the key catalytic residue, Gln204, in the active site. Following GTP hydrolysis, the loss of the γ-phosphate interactions causes the helix to disorder and the enzyme to be inactivated. As for HDC-8, electron density for the disordered helical region is lost, indicating that the region is truly disordered and does not take up a stable alternate conformation.

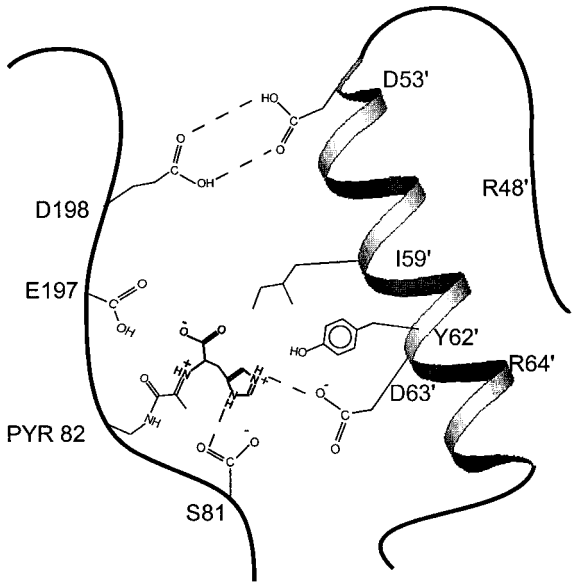

Figure 3. The active site region of HDC. The active site is formed at the interface of two monomers. The monomer on the left provides the pyruvoyl cofactor and catalytic acid E197. The substrate histidine is shown, in dark bonds, in a Schiff base complex with the pyruvoyl moiety. The monomer on the right contributes residues from the B helix that create the substrate binding pocket in the low pH, active form. At neutral or alkaline pH the helix disorders; at pH 8 the X-ray structure shows residues between R48′ and R64′ are disordered.

Enzyme activity of the α-amylase from *Bacillus licheniformis* is also controlled by a disorder/order transition.[18] In this case, metal ions trigger the transition. The enzyme is synthesized as an inactive apoenzyme in which residues 182 to 192 are totally disordered and 193 to 199 are α-helical. When the apoenzyme is secreted, it binds Ca ions that unwind the short helix and stabilize the region into a new loop conformation. The loop orders all the previously disordered residues and forms part of the polysaccharide binding site, thereby activating the enzyme.

In the case of *o*-succinylbenzoate synthase from *Escherichia coli*, it is the substrate that triggers a disorder/order transition.[19] When substrate binds to the enzyme, ionic interactions with part of the disordered region help stabilize residues 114 to 126 to form an α-helix. This structure becomes part of the regular motif of a $(\beta\alpha)_8$ barrel. The stabilizing of this helical segment brings a key residue, Lys133, into the active position for catalysis.

In summary, HDC is an enzyme that generates basic histamine to help control the acidification of the lactic acid-producing *Bacillus*. The enzyme is active at acidic pH, where it has a functional active site, partially formed by helix B from a neighboring molecule. As HDC's histamine product accumulates, the elevated pH pulls protons from the Asp198/Asp53′ trap. This causes the B helix to dis-

order, destroying the substrate-binding site and shutting off the enzyme. There are structural models of proteins regulated by pH in other ways, and models of enzymes where helix order/disorder controls activity in response to such effectors as phosphate, cations, or substrate. This appears to be the first structural analysis in which pH is used to control enzyme activity through helical stabilization.

Materials and Methods

Protein was isolated as described by Copelad *et al*.[10] Crystals were grown at room temperature by the hanging drop vapor diffusion method; drops contained 4 µl purified histidine decarboxylase (12.5 mg/ml), 1 µl *n*-dodecyl-β-D-maltoside (Hampton research) and 5 µl precipitant solution from the well (25% (w/v) PEG400, 8% PEG4000, 0.1 M Tris (pH 8.0), 0.1 M sodium acetate). Crystals were transferred in a loop directly from the drop to liquid nitrogen and then placed in the coldstream on the goniostat. X-ray diffraction data were collected at −170 °C using an MSC low temperature system, an RAXIS IV image plate detector and a Rigaku rotating anode X-ray generator operating at 50 kV and 100 mA. Data were collected in 40 minute exposures of 1.5 degree oscillations about the phi axis. The diffraction data were processed with the programs DENZO and SCALEPACK.[20]

Molecular replacement (MR) methods were used to phase the data. The model used was a tail-to-tail dimer of monomers from the structure of wild-type HDC at pH 4.8 (PDB i.d. 1PYA);[6] rotation and translation searches and Patterson correlation refinement were done using X-PLOR, and the initial model was refined using the slow cooling protocol of X-PLOR.[21] To facilitate manual rebuilding of the model, difference maps and LBEST-weighted $2F_o - F_c$ maps were prepared.[22] During refinement, omit maps of the form $(F_o - F_c)\alpha_{calc}$ were also calculated using X-PLOR. Further refinement was done with REFMAC.[23] Model building was done on a Silicon Graphics Indy computer using O.[24] MAPMAN[25] was used to help position bound solvent molecules.

Protein Data Bank atomic coordinates

The coordinates have been deposited with the RCSB Protein Data Bank. The PDB i.d. code is 1HQ6.

Acknowledgments

This work was supported by grant MCB-9601096 from the National Science Foundation, grant GM 30048 from the National Institutes of Health, and by grants from the Foundation for Research, and the Welch Foundation.

References

1. Recsei, P. A. & Snell, E. E. (1972). Histidine decarboxylaseless mutants of *Lactobacillus* 30a: isolation and growth properties. *J. Bacteriol.* **112**, 624-626.
2. Molenaar, D., Bosscher, J. S., Brink, B., Driessen, A. J. M. & Konings, W. N. (1993). Generation of a proton motive force by histidine decarboxylation and electrogenic histidine/histamine antiport in *Lactobacillus buchneri*. *J. Bacteriol.* **175**, 2864-2870.
3. van Poelje, P. D. & Snell, E. E. (1990). Pyruvoyl-dependent enzymes. *Annu. Rev. Biochem.* **59**, 29-59.
4. Recsei, P. A., Huynh, Q. K. & Snell, E. E. (1983). Conversion of prohistidine decarboxylase to histidine decarboxylase: peptide chain cleavage by non-hydrolytic serinolysis. *Proc. Natl Acad. Sci. USA,* **80**, 973-977.
5. Parks, E. H., Ernst, S. R., Hamlin, R., Xuong, Ng. H. & Hackert, M. L. (1985). Structure determination of histidine decarboxylase from *Lactobacillus* 30a at 3.0 Å resolution. *J. Mol. Biol.* **182**, 455-465.
6. Gallagher, T., Rozwarski, D. A., Ernst, S. R. & Hackert, M. L. (1993). Refined structure of pyruvoyl-dependent histidine decarboxylase from *Lactobacillus* 30a. *J. Mol. Biol.* **230**, 516-528.
7. Hackert, M. L., Meador, W. E., Oliver, R. M., Salmon, J. B., Recsei, P. A. & Snell, E. E. (1981). Crystallization and subunit structure of histidine decarboxylase from *Lactobacillus* 30a. *J. Biol. Chem.* **256**, 687-690.
8. Rashkovetskii, L. G. & Prozorovskii, N. V. (1983). Kinetic properties and functional role of domains of *Micrococcus* sp. n. histidine decarboxylase. *Biokhimiia,* **48**, 297-304.
9. Gallagher, T., Snell, E. E. & Hackert, M. L. (1989). Pyruvoyl-dependent histidine decarboxylase: active site structure and mechanistic analysis. *J. Biol. Chem.* **264**, 12737-12743.
10. Copeland, W. C., Vanderslice, P. & Robertus, J. D. (1987). Expression and characterization of *Lactobacillus* 30a histidine decarboxylase in *Escherichia coli*. *Protein Eng.* **1**, 419-423.
11. McElroy, H. E. & Robertus, J. D. (1989). Site-directed alteration of Glu197 and Glu66 in a pyruvoyl-dependent histidine decarboxylase. *Protein Eng.* **3**, 43-48.
12. Gelfman, C. M., Copeland, W. C. & Robertus, J. D. (1991). Site-directed alteration of four active site residues of a pyruvoyl-dependent histidine decarboxylase. *Biochemistry,* **30**, 1057-1062.
13. Pishko, E. J. & Robertus, J. D. (1993). Site-directed alteration of three active-site residues of a pyruvoyl-dependent histidine decarboxylase. *Biochemistry,* **32**, 4943-4948.
14. Pishko, E. J., Potter, K. A. & Robertus, J. D. (1995). Site-directed mutagenesis of intersubunit boundary residues in histidine decarboxylase, a pH-dependent allosteric enzyme. *Biochemistry,* **34**, 6069-6073.
15. Recsei, P. A. & Snell, E. E. (1970). Histidine decarboxylase of *Lactobacillus* 30a. VI. mechanism of action and kinetic properties. *Biochemistry,* **9**, 1492-1497.
16. Perutz, M. F., Kilmartin, J. V., Nishikura, K., Fogg, J. H., Butler, P. J. & Rollema, H. S. (1980). Identification of residues contributing to the Bohr effect of human haemoglobin. *J. Mol. Biol.* **138**, 649-668.
17. Mixon, M. B., Lee, E., Coleman, D. E., Berghuis, A. M., Gilman, A. G. & Sprang, S. R. (1995). Tertiary and quaternary structural changes in Gi alpha 1 induced by GTP hydrolysis. *Science,* **270**, 954-960.
18. Machius, M., Declerck, N., Huber, R. & Wiegand, G. (1998). Activation of *Bacillus licheniformis* alpha-amylase through a disorder → order transition of the substrate-binding site mediated by a calcium-sodium-calcium metal triad. *Structure,* **6**, 281-292.
19. Thompson, T. B., Garrett, J. B., Taylor, E. A., Meganathan, R., Gerlt, J. A. & Rayment, I. (2000).

Evolution of enzymatic activity in the enolase superfamily: structure of *o*-succinylbenzoate synthase from *Escherichia coli* in complex with Mg^{2+} and *o*-succinylbenzoate. *Biochemistry,* **39**, 10662-10676.
20. Otwinowski, Z. & Minor, W. (1997). Processing of X-ray diffraction data collected in oscillation mode. *Methods Enzymol.* **27**, 307-326.
21. Brünger, A. T. (1992). *X-PLOR version 3.1: a System for X-ray Crystallography and NMR*, Yale University Press, New Haven.
22. Urzhumtsev, A. G., Skovoroda, T. D. & Lunin, V. Y. (1996). A procedure compatible with X-PLOR for the calculation of electron-density maps weighted using an R-free-likelihood approach. *J. Appl. Crystallog.* **2**, 741-744.
23. Murshudov, G. N., Vagin, A. A. & Dodson, E. J. (1997). Refinement of macromolecular structures by the maximum-likelihood method. *Acta Crystallog. sect. D,* **53**, 240-255.
24. Jones, T. A., Zou, J. Y., Cowan, S. W. & Kjeldgaard, M. (1991). Improved methods for building models in electron density maps and the location of errors in these models. *Acta Crystallog. sect. A,* **47**, 110-119.
25. Kleywegt, G. J. & Jones, T. A. (1996). xdlMAPMAN and xdlDATAMAN - programs for reformatting, analysis, and manipulation of biomolecular electron-density maps and reflection data sets. *Acta Crystallog. sect. D,* **5**, 826-828.
26. Kraulis, P. J. (1991). MOLSCRIPT: a program to produce both detailed and schematic plots of protein structure. *J. Appl. Crystallog.* **24**, 946-950.

Edited by R. Huber

(Received 6 October 2000; received in revised form 21 December 2000; accepted 21 December 2000)